Article

A Screen of Cell-Surface Molecules Identifies

Leucine-Rich Repeat Proteins as Key

Mediators of Synaptic Target Selection

Mitsuhiko Kurusu, Amy Cording, Misako Taniguchi, Kaushiki Menon, Emiko Suzuki, and Kai Zinn

Supplemental Text

A Database of Cell-Surface and Secreted Proteins Involved in Cell Recognition

(Hynes and Zhao, 2000) and (Vogel et al., 2003) catalogued 366 *Drosophila* genes that encode putative CSS proteins containing nine types of extracellular (XC) domains. To define other CSS proteins that might be relevant to cell recognition, we searched the fly proteome with sequences of every domain in the "extracellular" portion of the SMART domain database (http://smart.embl-heidelberg.de/browse.shtml). We found a total of more than 80 domain types. We also catalogued G protein-coupled receptors (GPCRs) that have N-terminal protein-binding XC domains. We included glycosyltransferases (*e.g.* Fringe) and sulfotransferases (*e.g.* Pipe), which are necessary to create unique glycoproteins and proteoglycans. We also included proteins that contain no annotated domains but which were identified as CSS by their discoverers (*e.g*. Fog, Outstretched).

After creating the database, we removed several hundred proteins that we thought were unlikely to give unique phenotypes and/or be involved in muscle-neuronal signaling. These were usually members of large groups containing proteins with almost identical structures, including: small chitin-binding proteins, single-domain serine proteases, single-domain C-type lectins, protease inhibitors, and others. We did not include ion channels, pumps, transporters, secreted enzymes, and a variety of other classes of CSS proteins in the database. Our final CSS cell-recognition database (Supplementary Table 1) contains 976 proteins.

We then searched through all existing collections of UAS-containing EP-like lines and obtained insertions 5' to CSS database genes that could be used to drive their expression. These are: the original Rorth EP collection (Szeged), EY lines generated by the Bellen lab and the BDGP (Bloomington), GS lines (Kyoto Stock Center), GE/G lines (GenExel, Inc.), and WH and XP insertions generated by Exelixis, Inc. (Harvard). These insertions (462 total) should drive 410 of the 979 genes in the database, or over 40% of the cell recognition repertoire (Supplementary Tables 1 and 2).

Execution of the Screen

These 462 lines were all crossed to the *24B-GAL4* driver. Crosses were carried out at 29ºC. If F1 larvae did not emerge at 29ºC, the cross was repeated at 25ºC or 18ºC to reduce GAL4 activity. Wandering 3rd instar larvae were transferred into PBS and paralyzed on ice, then filleted and fixed as described below. Note that larvae should be kept with flaccid muscles while they are pinned for dissection, otherwise muscles become shortened, leading to tangled NMJs even in control crosses. Controls were F1 progeny from *UAS-GFP, 24B-Gal4* x w^{1118}. 10 confocal *z*-stacks were analyzed for each cross (10 A2 hemisegments from 5 F1 larvae).

Note that we do not know whether all of the EPs successfully drive protein expression. For most EPs that produced mistargeting phenotypes, we have analyzed normal expression by *in situ* hybridization and have also demonstrated that the mRNA for the gene downstream of the EP is in fact overexpressed in driver x EP embryos. For some of the genes, we had antibodies and could also determine whether protein was overexpressed. However, these EPs obviously represent a selected subset, and for those that did not produce phenotypes we have not examined whether they overexpress protein or mRNA.

Phenotypes Identified in the Screen

Supplementary Table 3 lists the set of 30 genes we identified as producing synaptic mistargeting phenotypes with a penetrance of ≥30%, and Figure 2 shows examples of phenotypes. The background penetrance of such phenotypes was <10%. The genes included in this set do not produce visible alterations in muscle fiber patterning or structure. Some genes produce loopback collaterals from 12 onto 13 (Figures 2C,D,I), while others produce mistargeting on muscle 6 (Figures 2F,G) or block outgrowth onto muscle 12 (Figure 2E).

Insertions for the 16 "new genes" (those not previously studied using genetics; indicated by CG numbers in Supplementary Table 3) within the group of 30 were then crossed to three other drivers: *G14-GAL4* (also early pan-muscle), *Mhc-GAL4* (late pan-muscle), and *Elav-GAL4* (pan-neuronal). Most of the lines tested so far produced the same phenotypes with similar penetrances with *G14-GAL4*, and did not generate phenotypes with *Elav-GAL4* (Supplementary Table 3). None produced phenotypes with *Mhc-GAL4*.

The muscle GOF screen had another purpose: to identify those CSS proteins whose overexpression in postsynaptic muscles causes alterations in the morphologies of NMJs without affecting the structures of the muscles themselves. We identified 55 genes that produce presynaptic terminal phenotypes with a penetrance of ≥60% when they are expressed in all muscles, and 28 other genes that generated phenotypes with ≥50% penetrance. These phenotypes include: larger boutons, smaller boutons, more boutons, fewer boutons, fused boutons, tangled NMJ arbors, clustered boutons, and dispersed boutons (Supplementary Figure 1, Supplementary Table 4).

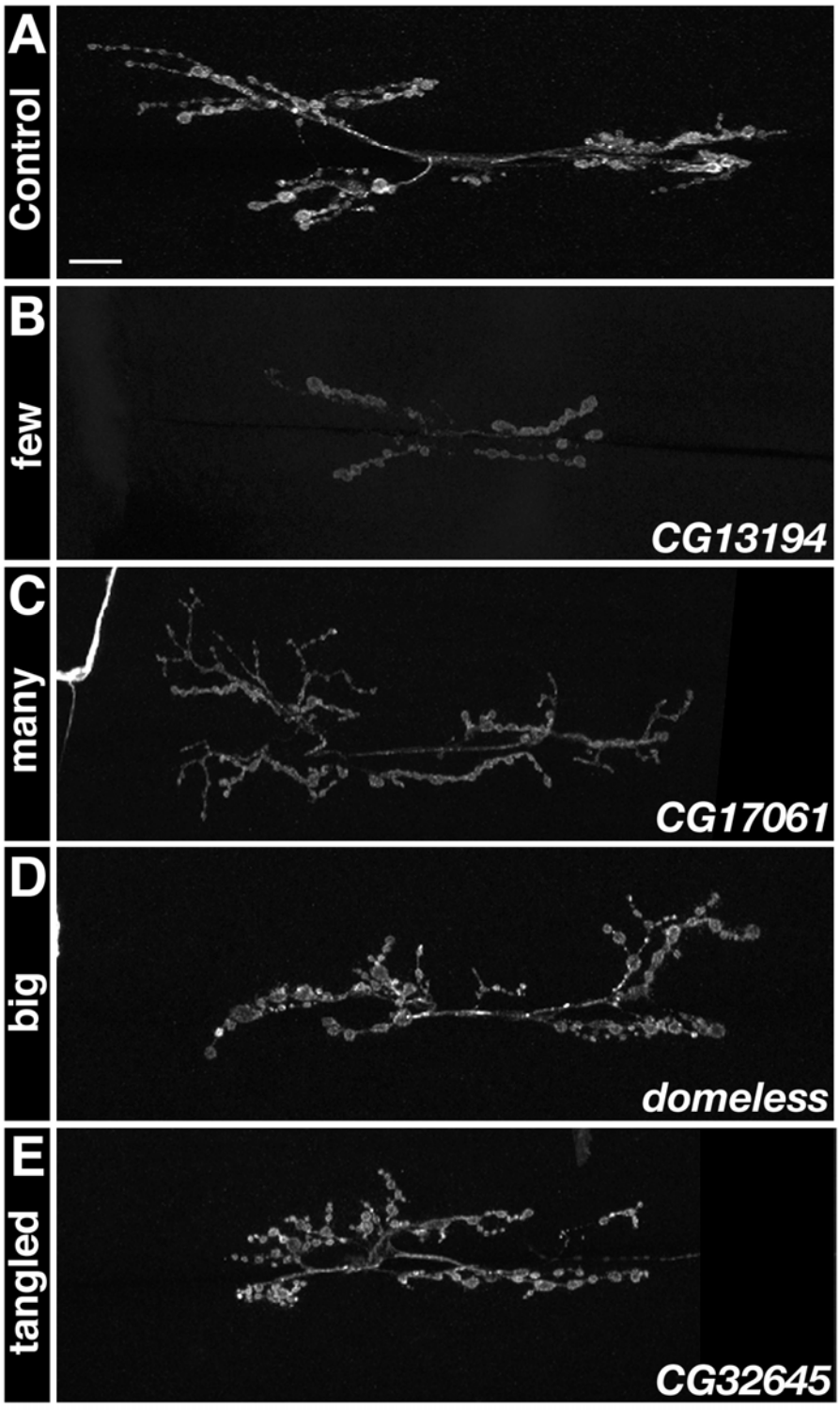
A
Control
B
few
CG13194
C
many
CG17061
D
big
domeless
E
tangled
CG32645

Figure S1. Examples of Synaptic Phenotypes
Confocal *z*-series images of the muscle 6/7 NMJ stained with 1D4 (white). Examples of the "few boutons" (B), "many boutons" (C), "big boutons" (D), and "tangled arbor" (E) phenotypes are shown. Gene names indicated on panels. Bar in (A), 20μm; applies to all panels.

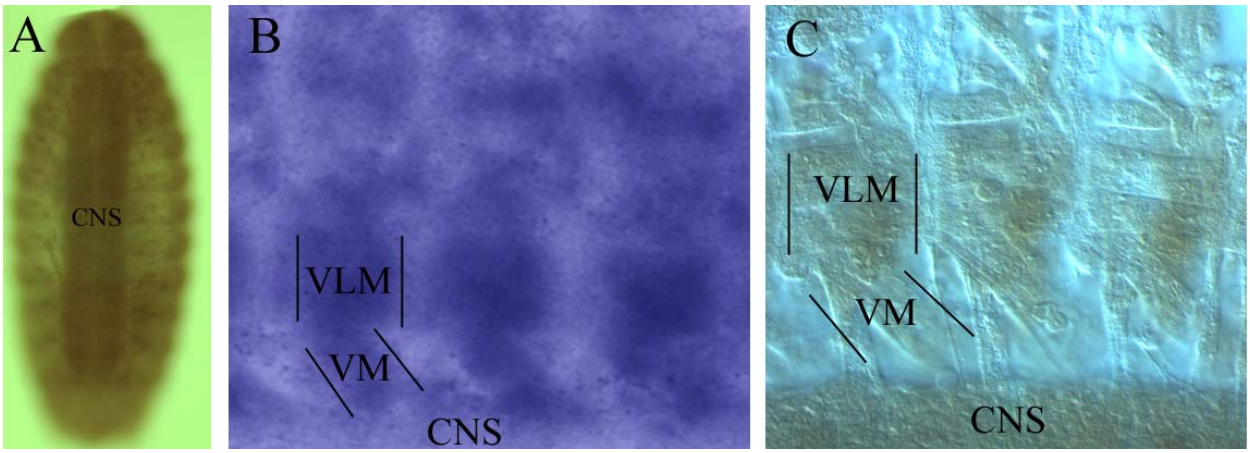

Figure S2. *haf/CG14351* Enhancer Trap and Protein Expression
(A) Protein expression, visualized by immunohistochemical staining (brown) with anti-Haf antibody in a stage 17 whole-mount embryo. The view is from the ventral side, and anterior is up. The CNS is indicated. Anterior is up and dorsal is to the left in (B) and (C). (B) Beta-galactosidase expression in a stage 16 embryo expressing *lacZ* from the NP0212 enhancer trap adjacent to the *haf* gene, visualized by X-gal staining. The VLM and ventral muscle (VM) regions are indicated in one segment, so that their characteristic shapes can be seen in the other segments. (C) Protein expression, in a stage 16 embryo fillet stained with anti-Haf antibody. The VLM and VM regions are indicated in one segment. The staining observed in these regions in (C) may correspond to the enhancer trap expression in (B).

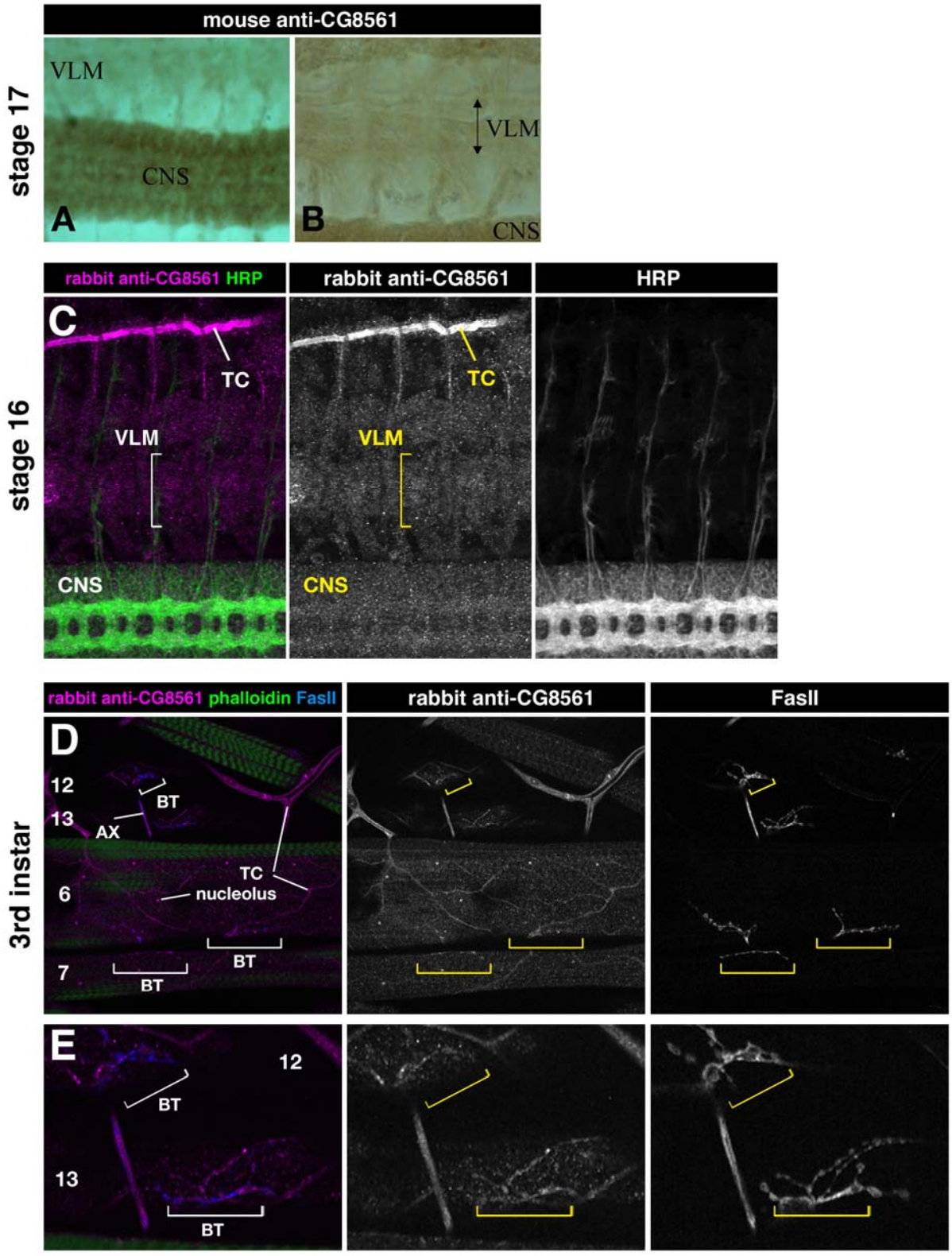
stage 17
mouse anti-CG8561
VLM
CNS
A
VLM
CNS
B
stage 16
rabbit anti-CG8561 HRP
rabbit anti-CG8561
HRP
C
TC
VLM
CNS
TC
VLM
CNS
3rd instar
rabbit anti-CG8561 phalloidin FasII
rabbit anti-CG8561
FasII
D
12
13
AX
BT
TC
nucleolus
6
7
BT
BT
E
12
13
BT
BT

Figure S3. CG8561 Protein Expression

(A) A filleted stage 17 embryo stained with mouse anti-CG8561. CNS staining is evident, and there may be weak staining in the VLMs, as they are darker than the ventral epidermis and ventral muscles which lie between them and the CNS. (B) A detail of a stage 17 embryo fillet stained with the antibody. The VLM region is indicated. (C) A single confocal section showing CG8561 protein recognized by the rabbit anti-peptide antibody (magenta/white) and the neuronal HRP epitope (green/white) in a stage 16 embryo fillet. Note that CG8561 is expressed at high levels on the dorsal tracheal trunk (arrow) and at lower levels on the ventrolateral muscles (bracket) and CNS. Embryos were stained with the rabbit anti-synthetic CG8561 peptide antibody. (D) A single confocal section showing CG8561 expression on 3rd instar NMJs. VLMs (12, 13, 6, 7) are in focus. Rabbit anti-CG8561 (magenta/white); phalloidin (green); anti-FasII (mAb 1D4; blue/white). The CG8561 antibody stained muscles, axonal shafts, boutons (indicated by brackets), tracheae, and nucleoli. A higher magnification view focusing on the m12 and m13 NMJs is shown in (E). BT, boutons; AX, axons; TC, tracheae.

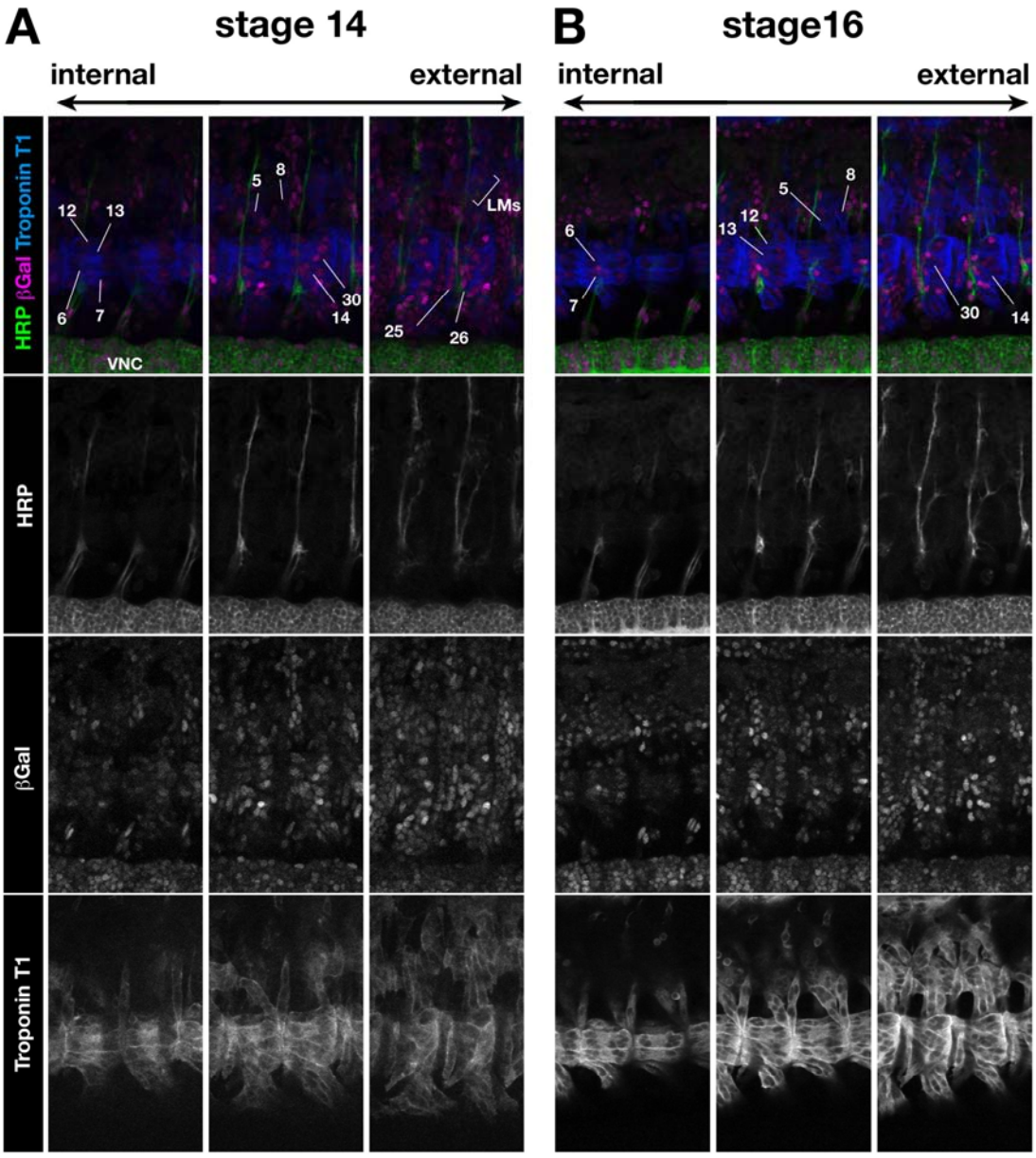
A
stage 14
internal
external
HRP βGal Troponin T1
12
13
6
7
VNC
5
8
30
14
LMs
25
26
HRP
βGal
Troponin T1
B
stage16
internal
external
6
7
13
12
5
8
30
14

Figure S4. Trn Promoter-Driven Nuclear Beta-Galactosidase Expression in Ventrolateral Muscles
A series of single confocal sections, from internal (muscle 6/7 layer), to middle (muscles 12 and 13), to external (muscles 14, 30, 28 (ISNb-innervated), and also 25, 26, and 27 (SNc-innervated)). (A) Late stage 14/early stage 15. (B) Early stage 16. Top panels, triple label for neuronal HRP epitope (green), beta-galactosidase (magenta), and muscle marker troponin T1 (blue). Single channels are shown separately (white signals) in the lower panels. Brackets indicate lateral muscles (21-24). VNC, ventral nerve cord.

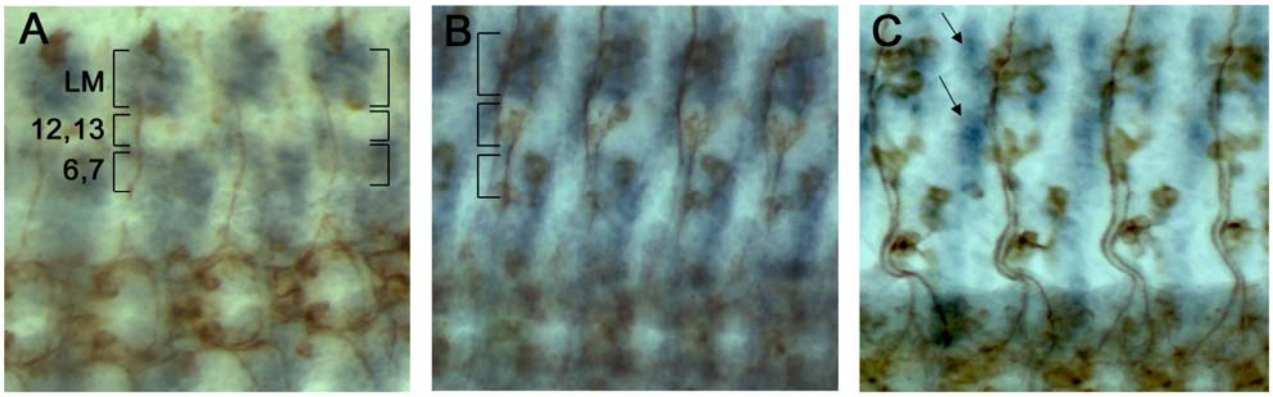

Figure S5. Trn Protein Expression in Embryonic Muscles
(A-C) Expression of Trn protein at late stage 14/early stage 15 (A), early stage 16 (B), and late stage 16 (C). Embryos were double stained for Trn (blue) and 22C10 antigen (labels the PNS; brown) using HRP immunohistochemistry. Brackets in (A) and (B) indicate the locations of the lateral muscles (LM), muscles 12 and 13, and muscles 6 and 7; these regions were defined using PNS cell body position as a guide. Note that Trn staining is not seen in the m12,13 region. By late stage 16 (C), Trn expression is gone from patches and replaced by stripes (arrows), which may be muscle attachment sites.

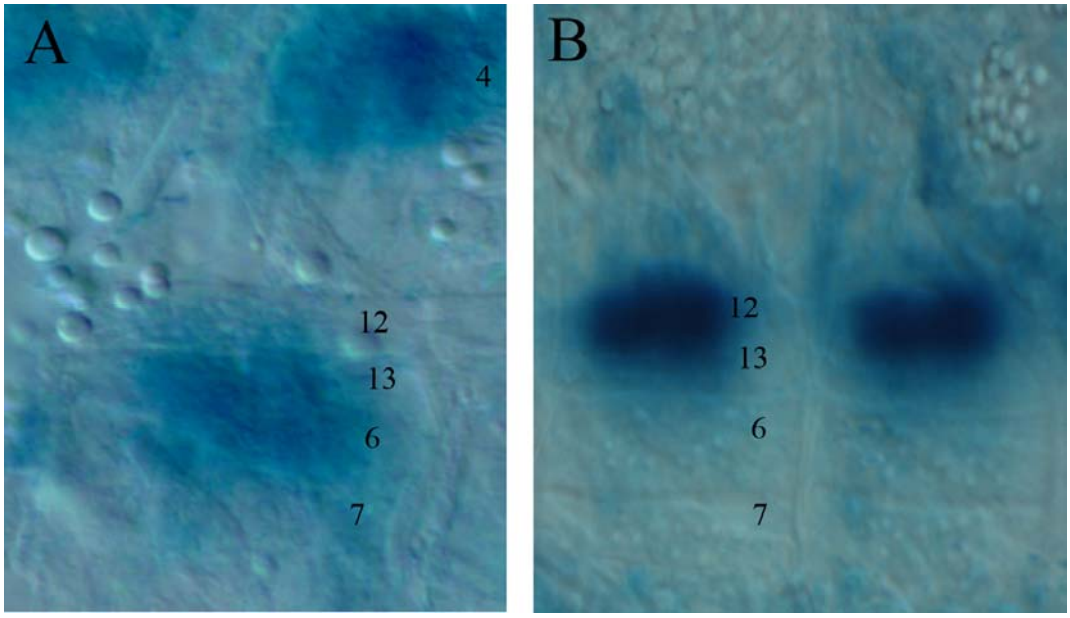

Figure S6. Expression Patterns of the H94 and 5053A GAL4 Drivers
Stage 16 embryo fillets are shown. X-gal staining (blue) was used to visualize *lacZ*-expressing muscles in driver x UAS-cytoplasmic *lacZ* embryos. (A) H94 expresses at a lower level than 5053A in muscles 13, 6, and 4, and weak staining is observed in muscle 12. (B) 5053A expresses only in muscle 12.

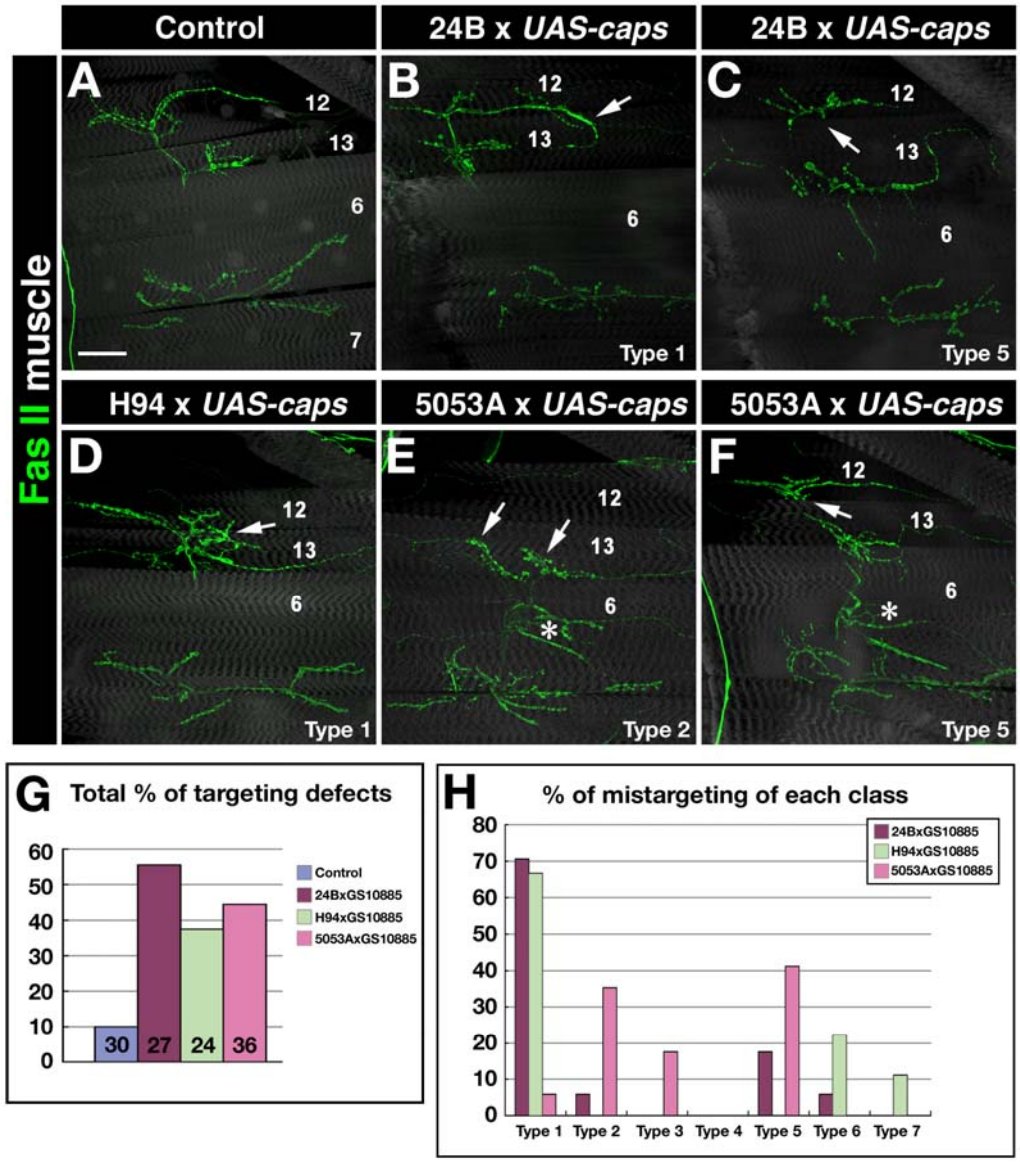

Figure S7. Phenotypes Produced by Muscle Overexpression of Caps
Confocal *z*-series images of 3rd instar F1 larvae stained with 1D4 (green) and Alexa-488-phalloidin or UAS-GFP expression (gray). (A) Control (*UAS-GFP, 24B-GAL4 x w*). The NMJs on muscle 6/7, 13, and 12 are evident. (B-C) 24B-driven expression of *UAS-Caps* (a transgenic cDNA construct from A. Nose). Arrow in (B), loopback branch onto 13 (Type 1). Arrow in (C), gap in the ISNb nerve, showing that it travels under muscle 13 rather than over it (Type 5). (D) H94-driven expression of UAS-Caps. Arrow, a portion of the muscle 12 NMJ arbor that has expanded onto 13 (Type 1). (E-F) 5053A (muscle 12-only)-driven expression of UAS-Caps. Arrows in (E), branches on m13 that have failed to reach muscle 12 (Type 2). Arrow in (F), gap in the ISNb nerve, showing that it travels under muscle 13 rather than over it (Type 5). In this case the NMJ on m13 extends upward along the muscle, almost to the 12/13 border, so the gap is small, but the m12 and m13 NMJs are unconnected over the top of m13. Asterisks in (E) and (F), normal NMJs on m30/14. (G) Bar graph of % targeting defects seen with the three drivers, *vs*. *24B* driver x UAS-GFP control. (H) Distribution of phenotypic types seen with the three drivers. Note that

~70% of targeting errors with *24B* and *H94* are Type 1 (12→13 loopback); *24B* data match results in previously published work (Shishido et al., 1998). By contrast, ~75% of targeting errors with muscle 12-only driver are Type 2 (no m12 innervation) and Type 5 (growth under m13 rather than over it), exactly as observed for Trn overexpression in Figure 4.

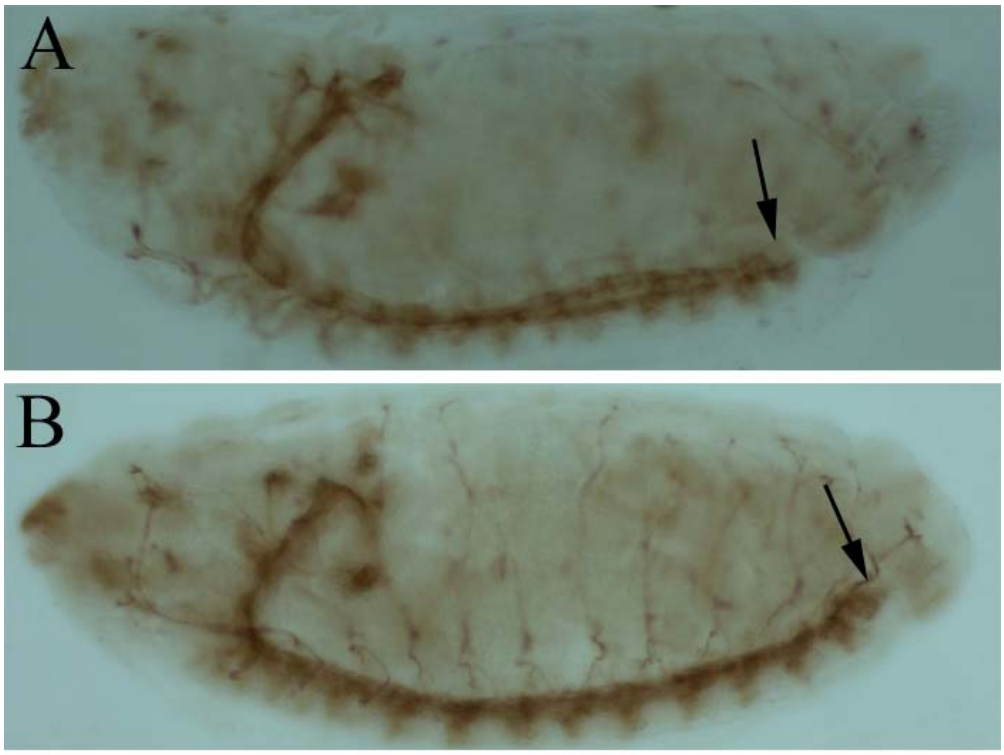

Figure 8. Pancellular CG8561 RNAi Causes a Failure of Nerve Cord Condensation
(A) A side view of a late stage 16 control embryo stained with mAb 1D4. The posterior end of the CNS, which has partially condensed by this time, is indicated by an arrow. (B) A side view of a late stage 16 CG8561 RNAi x *tub-GAL4* embryo. Note that the posterior end of the CNS (arrow) is much closer to the posterior end of the embryo (as in a stage 14 or 15 embryo), indicating that nerve cord condensation fails to occur in pancellular CG8561 RNAi embryos.

Supplemental References

Hynes, R. O., and Zhao, Q. (2000). The evolution of cell adhesion. J Cell Biol *150*, F89-96.
Shishido, E., Takeichi, M., and Nose, A. (1998). Drosophila synapse formation: regulation by transmembrane protein with Leu-rich repeats, CAPRICIOUS. Science *280*, 2118-2121.
Vogel, C., Teichmann, S. A., and Chothia, C. (2003). The immunoglobulin superfamily in Drosophila melanogaster and Caenorhabditis elegans and the evolution of complexity. Development *130*, 6317-6328.